

# Downward uniformity and optical properties of porous silicon layers\*

Long Yongfu(龙永福)<sup>1,†</sup> and Ge Jin(葛进)<sup>2</sup>

(1 Department of Physics and Electronics, Hunan University of Arts and Science, Changde 415000, China)

(2 National Key Laboratory for Surface Physics, Fudan University, Shanghai 200433, China)

**Abstract:** Porous silicon (PS) samples were fabricated by pulse current etching using different times. The downward uniformity and optical properties of the PS layers have been investigated using reflectance spectroscopy, photoluminescence spectroscopy, and scanning electron microscopy (SEM). The relationship between the refractive index and the optical thickness of PS samples and the etching depth has been analyzed in detail. As the etching depth increases, the average refractive index decreases, indicating that the porosity becomes higher, and the formation rate of the optical thickness decreases. Meanwhile, the reflectance spectra exhibit less intense interference oscillations, which mean the uniformity and interface smoothness of the PS layers become worse. In addition, the intensity of PL emission spectra is slightly increased.

**Key words:** porous silicon; uniformity; optical properties; photoluminescence

**DOI:** 10.1088/1674-4926/30/5/052003

**PACC:** 6800; 7865

## 1. Introduction

Since the discovery of porous silicon (PS) photoluminescence (PL) at room temperature in 1990 by Canham *et al.*<sup>[1]</sup>, it has attracted the interest of many researchers<sup>[2–9]</sup>, especially due to its potential application fields<sup>[7–14]</sup>, such as electroluminescence (EL), lasers, and optical microcavities. In 1996, the realization of silicon-based visible light-emitting prototype devices<sup>[15]</sup> integrated into microelectronic circuits was a major milestone for the applied research on PS. However, in order to realize PS optical devices with excellent quality, the optical parameters, such as the refractive index ( $n$ ) and the optical thickness ( $nd$ ), must be accurately controlled. Previous works<sup>[3–6]</sup> have concentrated on the effects of anodic parameters on the microstructure and optical properties of the whole PS layer, resulting in a lot of valuable experimental rules. In general, the refractive index or porosity is only dependent on the etching current density under the same conditions<sup>[4]</sup> which include the composition of the electrolyte, the etching temperature, and the resistivity and conduction type of the Si wafer. Therefore, the refractive index or porosity can be controlled by changing the etching current density, resulting in realization of optical PS devices, such as microcavities and distributed Bragg reflectors (DBRs). Pavesi *et al.*<sup>[11]</sup> were the first group to report that the PS multilayers can be used to fabricate optical microcavities by stacking high refractive index layers and low refractive index layers periodically. In 2002, Reece *et al.*<sup>[13]</sup> fabricated high-quality PS optical microcavities with an optical resonance in the near infrared range and a line width of 0.63 nm. The PS microcavities fabricated by the aforementioned groups<sup>[11–13]</sup>, had a different full width at half maxima (FWHMs) indicating that the device quality depends on

the optical parameters of the PS layers. However, a theoretical simulation of the PS microcavity<sup>[13]</sup> predicts that even a resonance line width of 0.1 nm can be emitted. The theoretical expectation has not been realized in previous experiments. The quality of the PS layers is still far from satisfactory for device applications. One of the primary problems arises from the uniformity and smoothness of the PS layer. In 2005, Ghulinyan *et al.*<sup>[16]</sup> researched the time-resolved optical Bloch oscillations in porous silicon superlattice structures by controlling the linear gradient of the refractive index along the growth direction.

In order to obtain better optical properties of the PS layers with more uniform and smoother interfaces, Hou *et al.*<sup>[17]</sup> and Liu *et al.*<sup>[18]</sup> have, respectively, reported on the pulse electrochemical etching technique and the ultrasonic etching method. These techniques result in more uniform PS layers with smoother interfaces than those prepared by the direct current etching technique. Recently, Ge *et al.*<sup>[19]</sup> have studied the influence of the pulse current on the uniformity and the optical properties of PS layers. These studies have obtained many valuable results; however, they have not systematically studied the downward uniformity and the optical properties of PS layers along the vertical direction. It is well known that the quality of PS optical devices, such as microcavities and distributed (DBR), is determined by the uniformity and the interface smoothness of the PS layers. Therefore, it is necessary to systematically investigate the effect of the downward uniformity and the interface smoothness of the PS layer on the etching depth.

In this work, we systematically demonstrate that the downward uniformity and the optical properties of PS layers strongly depend on the etching process. At a constant current

\* Project supported by the National Natural Science Foundation of China and the Natural Science Foundation of Hunan Province (No. 04JJ40031).

† Corresponding author. Email: yongfulong@163.com

Received 11 November 2008, revised manuscript received 17 December 2008

© 2009 Chinese Institute of Electronics

density of  $60 \text{ mA/cm}^2$ , reducing the etching times from 4 to 1 min results in more uniform layers and smoother interfaces, and an increase of the refractive index from 1.79 to 2.03. In addition, the PL intensity of the PS is slightly decreased, and a blue-shift of the PL envelope curves is observed.

## 2. Experiment

In our experiments, the used wafer was (100)-oriented, highly-doped p-type silicon with a low resistivity ( $0.007\text{--}0.01 \text{ }\Omega\text{-cm}$ ), and coated with an aluminum layer on the back. The wafer was annealed to provide a low resistance ohmic electrical contact. Each sample was cut into pieces with an edge length of 15 mm. Each sample was mounted onto a sample holder. All PS samples were fabricated at  $25 \text{ }^\circ\text{C}$  by PC-controlled pulsed electrochemically etching<sup>[17]</sup> in an electrolyte ( $\text{HF}(40\%) : \text{ethanol} : \text{H}_2\text{O} = 1 : 1 : 2$  by volume). Four samples, denoted as A, B, C, and D, were prepared in the dark at different etching times of 1, 2, 3, and 4 min, respectively. The current density was set to be  $60 \text{ mA/cm}^2$  with a repetition rate of 200 Hz and a duty cycle of 0.5 resulting in sponge-like PS structures of different thicknesses of  $1\text{--}5 \text{ }\mu\text{m}$ . After etching, each PS sample was dipped into ethanol at  $25 \text{ }^\circ\text{C}$ , then rinsed in de-ionized water, and finally dried in ambient air.

The prepared PS samples were characterized by reflectance spectroscopy, PL spectroscopy and scanning electron microscopy (SEM). The reflectance spectra with an incidence angle of  $10^\circ$  were taken by using a white light source (tungsten halogen lamp). For the PL spectra, a 405 nm light beam from a semiconductor laser with a power of 10 mW and a spot size of about  $1 \text{ mm}^2$  was used. The PL measurements were carried out using the same detection apparatus as used for the reflectance measurements. The SEM measurements were performed with a PHILIPS XL30 FEG. The refractive index  $n$  was obtained as the ratio of the optical thickness  $nd$ , resulting from highly accurate reflectance spectra measured at a wavelength of about 700 nm, to the physical thickness  $d$ , obtained from cross-section SEM measurements.

## 3. Results and discussions

The reflectance spectra of PS samples A, B, C, and D, prepared by using different etching times, are shown in Fig. 1 as curves *a*, *b*, *c*, and *d*, respectively. As shown in the figure, intensity oscillations appear over the wavelength range of 450–850 nm. These oscillations result from the optical interference between the light beams reflected from the top and bottom interfaces of the PS layers. All four samples exhibit strong oscillations at a wavelength of 790 nm, but the oscillation amplitude  $\Delta R$  decreases with decreasing wavelength  $\lambda$ . The rates, at which the amplitude decreases, is sample dependent: for sample D etched for 4 min, the oscillations almost disappears for wavelength less than 500 nm; but for sample A etched for 1 min, the oscillations remain almost unchanged over the whole wavelength range, as shown in the figure. At a short wavelength of 540 nm, the ratios ( $\Delta R/R$ ) of the

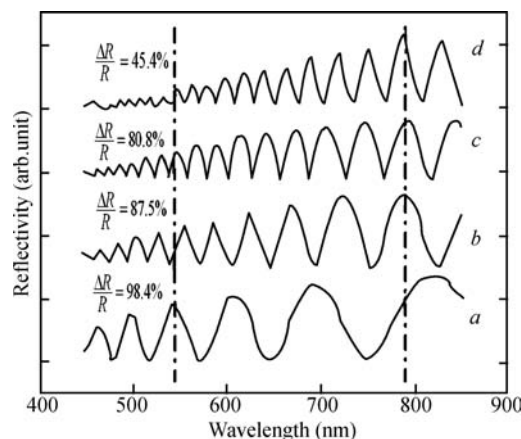


Fig. 1. Reflectivity spectra of PS samples A, B, C, and D corresponding to curves *a*, *b*, *c*, and *d*, respectively.

oscillation amplitude ( $\Delta R$ ) to the maximum reflectance intensity ( $R$ ) are 98.4%, 87.5%, 80.8%, and 45.4%, for samples A, B, C, and D, respectively, as shown in Fig. 1. This indicates that the ratio ( $\Delta R/R$ ) decreases with increasing etching time and, thus, etching depth. The data shows that a reduced etching time will lead to more pronounced interferences. In general, the interference intensity of a mono-layer depends on the uniformity of the layer and the smoothness of the top and bottom interfaces. Therefore, the present experimental results show that sample A, etched for 1 min, is the most uniform sample with the smoothest surfaces and interfaces. In addition, in the wavelength range from 540 to 790 nm (indicated by two vertical dotted lines in Fig. 1), there exist 2.75 oscillation periods in curve *a*, and 5.5, 8, and 10 oscillation periods in curves *b*, *c*, and *d*, respectively. Different oscillation periods reflect different optical thicknesses of the samples. From the maxima in the reflectance spectra of the PS samples, the optical thickness ( $nd$ ) can be calculated by the Fabry–Perot equation<sup>[14]</sup>:  $nd = \frac{\lambda_r + \lambda_r}{2(\lambda_{r+1} - \lambda_r)}$ , where  $d$  and  $n$  are, respectively, the physical thickness and the refractive index of the PS layer, while  $\lambda_r$  is the wavelength of the  $r$ -th reflectance maximum. The optical thicknesses ( $nd$ ) are obtained as 2560, 4730, 6650, and 8540 nm for samples A, B, C, and D, respectively, at around the wavelength of 700 nm, indicating that the optical thickness increases with etching time. However, the value, by which the optical thickness increases per unit time, decreases during the etching process; the formation rate of the optical thickness decreases from 2560, 2170, 1920, to 1890 nm/min for etching in the first, second, third and fourth minute, respectively. The above results show that a shorter etching time is beneficial for improving the downward uniformity and the interface smoothness of a PS layer, and it increases the average variation ratio of the optical thickness and weakens the lateral etching ability. The fact that the formation rate of the optical thickness decreases during the etching process can be explained as follows: the physical thickness of a PS layer increases with etching time, resulting in the diffusion of reaction products away from PS pores and the diffusion of HF into the pores more difficult. The HF concentration in the pores at the Si–PS interface is, thus, not equivalent to the concentration in the electrolyte.

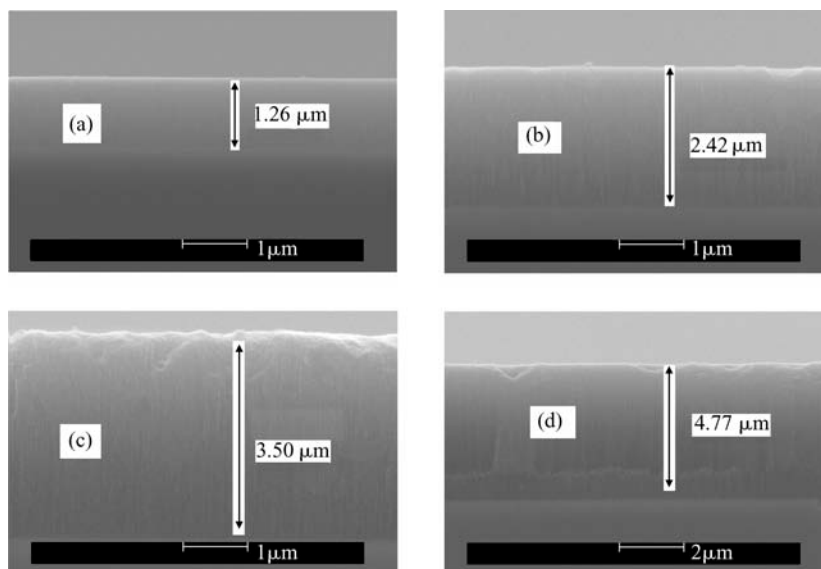


Fig. 2. SEM images taken from the cross-section of PS (a) sample A, (b) sample B, (c) sample C, and (d) sample D.

Namely, the  $F^-$  concentration decreases along the vertical direction, resulting in the lateral etching effect<sup>[4]</sup>. This effect leads to an increase of the porosity and to a decrease of the refractive index along the vertical direction. These results demonstrate that a decreasing etching time is beneficial for improving the uniformity and the interface smoothness of PS layers. Accordingly, decreasing the duty cycle of the pulse etching waveform would be an efficient way<sup>[19]</sup> to fabricate high-quality multilayer optical devices, such as PS microcavities and distributed DBRs.

Although the optical thickness of the PS layer can be calculated from the interference data of the reflectance spectra, the physical thickness of each sample is measured directly by SEM. The SEM images of the cross-sections of the four samples are presented in Fig. 2 as panels (a), (b), (c), and (d). As shown in Fig. 2, the physical thicknesses of samples A, B, C, and D are 1.26, 2.42, 3.50, and 4.77  $\mu\text{m}$ , respectively. In the present experiment, all four samples were etched with a current density of 60  $\text{mA}/\text{cm}^2$  for 1, 2, 3, and 4 min, and corresponding instantaneous formation rates of 1.26, 1.16, 1.08, and 1.27  $\mu\text{m}/\text{min}$ , respectively. Therefore, within the experimental error, it can be said that the physical formation rate is independent of time. The reason that the vertical formation rate of the PS layers is almost constant with etching time might be that the anode provides a constant amount of holes to the Si atoms at the bottom of the micropores per unit time. Since a constant current density is used in the present experiment, the  $F^-$  in the pores can react very easily with Si atoms at micropores bottoms, leading to a constant vertical etching ability.

Combining the physical thickness measurements by SEM with the optical thickness determined from the oscillations of the reflectance spectra, the average refractive index  $n$  was calculated to be 2.03, 1.95, 1.90, and 1.79 for samples A, B, C, and D, respectively. The results show that a larger physical thickness leads to a smaller refractive index or a higher porosity along the vertical direction. Figure 3 shows the dependence of the average refractive index of the PS layer on

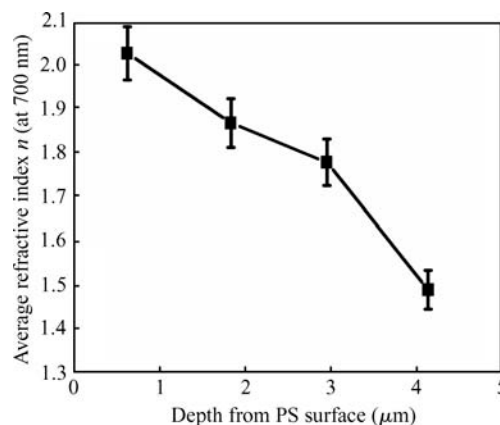


Fig. 3. Average refractive index of PS fabricated at  $J = 60 \text{ mA}/\text{cm}^2$  versus the depth from the PS surface when using HF (40%) :  $\text{C}_2\text{H}_5\text{OH}$  :  $\text{H}_2\text{O} = 1 : 1 : 2$  (in volume).

the etching depth. It is seen that the average refractive index of PS layers formed in the first, second, third to fourth minute decreases from 2.03, 1.87, 1.78, to 1.49, respectively, as the depth increases. This shows that in etching process the vertical physical etching rate of the PS layer is almost constant, but the lateral erosion increases; meanwhile, the formation rate of the optical thickness of the PS layer is decreased, resulting in a worse downward uniformity and less interfaces smoothness. This phenomenon can be explained by the following mechanism: as the physical thickness of a PS layer increases, the diffusion of HF into the pores is decreased, resulting in a gradient of the  $F^-$  concentration along the vertical direction. This facilitates the laterally erosion on the micropore walls<sup>[4]</sup> and results in larger pore diameters and, thus, an increased porosity. In addition, during the electrochemical etching process, hydrogen bubbles will be produced in the PS layer. This leads to a concentration gradient with the lowest HF concentration and the highest hydrogen concentration at the bottom of PS pores. Thus, the resistance in the etching process goes up, which was also observed in the previous paper<sup>[17]</sup>. During the period of a single pulse, the constant current density results in a

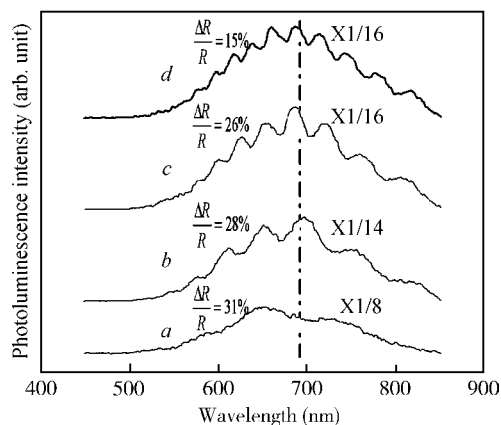


Fig. 4. Photoluminescence spectra of samples A, B, C and D corresponding to curves *a*, *b*, *c* and *d*, respectively.

constant vertical etching rate. As the resistance of the etching electrolyte increases<sup>[17]</sup>, the electric field in the PS layer increases along the vertical direction. This leads to the excitation of a lot of holes in the side walls of the micropores and, thus, form a gradient of holes. The highest holes concentration exists at the bottom of the micropores, but the  $F^-$  ions react with the Si atoms in the side walls to form Si-F bonds, thus also increasing the lateral etching. This results in an increase of the porosity and a decrease of the refractive index along the vertical direction. The results demonstrate that the uniformity of the PS layer becomes worse during the etching process, namely, the refractive index decreases and the porosity increases along the vertical direction.

PL spectra of the PS samples A, B, C, and D are shown in Fig. 4. One can see that the PL intensity slightly increases with etching time. The ratio of the PL intensity of the four samples (A, B, C, D) is approximately 8 : 14 : 16 : 16. Such a phenomenon is consistent with the fact that the porosity increases with increasing etching depth. Furthermore, the oscillations of the PL spectra of the four samples can be seen in Fig. 4. The ratios ( $\Delta R/R$ ) (the position of the vertical dotted lines in Fig. 4) of the oscillation amplitude ( $\Delta R$ ) to the maximum PL intensity ( $R$ ) are 31%, 28%, 26%, and 15%, respectively. The interference intensity, thus, decreases with increasing etching depth. This result again demonstrates that shortening the etching time can improve the uniformity and the interface smoothness of the PS layers. Besides, the peaks of the envelope curves of the PL spectra in Fig. 4 exhibit a trend of red-shift with increasing etching depth, which results from an average increase of the porosity or a decrease of the refractive index.

The dependence of the downward uniformity and the optical properties of PS layers on the etching depth have been investigated. The above experimental results demonstrate that under otherwise constant etching conditions, a shorter etching time leads to a thinner, more uniform PS layer with smoother interfaces, lower porosity, and higher refractive index. In order to accurately control the refractive index in a multilayer stack, decreasing the pulse width and the duty cycle would be an efficient way.

## 4. Conclusion

In conclusion, the etching time affects the downward uniformity and optical properties of PS layers. The refractive index of PS layers decreases along the vertical direction, indicating higher porosity. In order to obtain a more uniform PS layer with smoother interfaces, narrower electric pulses should be used.

## Acknowledgements

The authors would like to thank Prof. Hou X. Y. and Prof. Ding X. M. for their fruitful instructions and discussions, and are indebted to Dr. Li N. and Dr. Yang H. B. for useful assistance during the experiments.

## References

- [1] Canham L T. Silicon quantum wire array fabrication by electrochemical and chemical dissolution of wafers. *Appl Phys Lett*, 1990, 57: 1046
- [2] Lehmann V, Gösele U. Porous silicon formation: a quantum wire effect. *Appl Phys Lett*, 1991, 58: 856
- [3] John G C, Singh V A. Porous silicon: theoretical studies. *Phys Rep*, 1995, 263: 93
- [4] Bisi O, Ossicini S, Pavese L. Porous silicon: a quantum sponge structure for silicon based optoelectronics. *Surf Sci Rep*, 2000, 38: 1
- [5] Dian J, Macek A, Nižňský D, et al. SEM and HRTEM study of porous silicon-relationship between fabrication, morphology and optical properties. *Appl Surf Sci*, 2004, 238: 169
- [6] Ge J, Yin W J, Long Y F, et al. Positive and negative pulse etching method of porous silicon fabrication. *Chin Phys Lett*, 2007, 24: 1361
- [7] Koshida N, Koyama H. Visible electroluminescence from porous silicon. *Appl Phys Lett*, 1992, 60: 347
- [8] Pavese L, Ceschini M, Mariotto G, et al. Spectroscopic investigation of electroluminescent porous silicon. *J Appl Phys*, 1994, 75: 1118
- [9] Ghulinyan M, Oton C J, Bonetti G, et al. Free-standing porous silicon single and multiple optical cavities. *J Appl Phys*, 2003, 93: 9724
- [10] Vincent G. Optical properties of porous silicon superlattices. *Appl Phys Lett*, 1994, 64: 2367
- [11] Pavese L, Mazzoleni C, Tredicucci A, et al. Controlled photon emission in porous silicon microcavities. *Appl Phys Lett*, 1995, 67: 3280
- [12] Xu S H, Xiong Z H, Gu L L, et al. Photon confinement in one-dimensional photonic quantum-well structures of nanoporous silicon. *Solid State Commun*, 2003, 126: 125
- [13] Reece P J, Léronnel G, Zheng W H, et al. Optical microcavities with subnanometer linewidths based on porous silicon. *Appl Phys Lett*, 2002, 81: 4895
- [14] Mazzoleni C, Pavese L. Application to optical components of dielectric porous silicon multilayers. *Appl Phys Lett*, 1995, 67: 2983
- [15] Hirschman K D, Tsybeskov L, Dutttagupta S P, et al. Silicon-based visible light-emitting devices integrated into microelectronic circuits. *Nature*, 1996, 384: 338

- [16] Ghulinyan M, Oton C J, Gaburro Z, et al. Time resolved optical Bloch oscillations in porous silicon superlattice structures. *Phys Status Solidi*, 2005, 9: 3283
- [17] Hou X Y, Fan H L, Xu L, et al. Pulsed anodic etching: an effective method of preparing light-emitting porous silicon. *Appl Phys Lett*, 1996, 68: 2323
- [18] Liu Y, Xiong Z H, Liu Y, et al. A novel method of fabricating porous silicon material: ultrasonically enhanced anodic electrochemical etching. *Solid State Commun*, 2003, 127: 583
- [19] Ge J, Yin W J, Ma L L, et al. Systematic study on pulse parameters in fabricating porous silicon-layered structures by pulse electrochemical etching. *Semicond Sci Tech*, 2007, 22: 925